

# Fracture Toughness and Shear Yield Strength Determination for Two Selected Species of Central European Provenance

Lud'ka Hlášková,<sup>a,\*</sup> Kazimierz A. Orlowski,<sup>b</sup> Zdeněk Kopecký,<sup>a</sup> Martin Sviták,<sup>a</sup> and Tomasz Ochrymiuk<sup>c</sup>

When offcut of wood is formed by shearing, Atkins's analyses of sawing processes can be applied. Using this modern approach, it is possible to determine the fracture toughness and shear yield strength of wood. This model is only applicable for the axial-perpendicular cutting direction because both of these parameters are suitable for the given direction of cutting edge movement and cannot be considered material constants. Alternatively, these parameters can be recalculated for the perpendicular and axial directions of cutting when the parameters are considered non-variable quantities. The set of data necessary for calculation can be easily obtained while cutting wood with common circular saw blades. It is necessary to ensure a minimum of two levels of workpiece height and two diverse levels of feed speed. The main aim was to develop an alternative methodology for simultaneous determination of wood fracture toughness and shear yield strength for two principal directions regarding wood grains on the basis of cutting tests performed during circular saw blade cutting for two selected wood species of Central Europe provenance, such as spruce (*Picea abies* (L.) Karst.) and beech (*Fagus sylvatica* L.).

*Keywords:* Fracture toughness; Shear yield strength; Wood cutting; Circular saw blade

*Contact information:* a: Department of Wood Processing Technologies, Faculty of Forestry and Wood Technology, Mendel University in Brno, Zemědělská 3, 613 00 Brno, Czech Republic; b: Department of Manufacturing Engineering and Automation, Faculty of Manufacturing Engineering, Gdansk University of Technology, Narutowicza 11/12, 80-233 Gdansk, Poland (ORCID id: 0000-0003-1998-521X); c: The Szewalski Institute of Fluid-Flow Machinery Polish Academy of Sciences, Centre of Flow and Combustion, Aerodynamics Department, Fiszera 14, 80-952 Gdansk, Poland (ORCID id: 0000-0002-6859-279X); \*Corresponding author: ludka.hlaskova@mendelu.cz

## INTRODUCTION

The removal of material includes fracture, which is the separation of parts of a material. In this context, the total energy is involved in material separation. In fragile solid materials, this energy is approximately as large as the free surface energy. The free surface energy of solids can be described as the degree of broken chemical bonds with the formation of a new surface (Bursikova *et al.* 2004). Machining of such materials cannot generally be understood as a cutting process, but rather a controlled crack propagation. In other material groups, energies other than the free surface energy participate in the creation of new surfaces. These irreversible processes associated with energy dissipation include plastic creep and accumulation of damage. Plastic creep is typical for malleable metals and polymers (isotropic, homogeneous), and accumulation of damage occurs particularly in multiphase composites (especially in fibrous ones), including wood (anisotropic, heterogeneous) (Jeronimidis 2000).

The energy-absorbing mechanisms associated with fracture and woodworking are diverse and include several levels of hierarchy: fracture and cellulose fibre damage, lignin-carbohydrate matrix disruption, separation and irreversible cell wall deformation, middle lamella disruption, and cellular structure collapse in shear and under pressure load. Wood in general exhibits brittle and linear-elastic behaviour under a short-term load. As a result, wood fracture can be considered in terms of linear elastic fracture mechanics (Parhizgar *et al.* 1982; Triboulot *et al.* 1984).

The question of whether or not fracture and crack propagation play a role in the cutting process has a complex history. Reuleaux (1900) was the first to deal with this issue. Reuleaux suggested, based on everyday experiences like potato peeling and wood splitting, that chips are created in the bending of all materials. For Reuleaux's theory, an observable crack in front of the cutting tool is required. There was a problem with the formation of chips of constant thickness. The crack tended to curve at the end of the thin chip towards the free surface. The material then broke off with a simultaneous crack propagation and discontinuous chip creation, especially with fragile and solid materials. Elastic bending is the only method for creating constant uncut chip thickness if the fracture toughness is parallel to the surface and smaller than in the other directions. This is the case in anisotropic materials that have different features in different directions (slate, mica, wood). This theory was abandoned afterwards because of its mentioned drawbacks.

Recently, the Reuleaux error has been corrected (Atkins 2003, 2005). With the application of the results based on fracture tests, further progress can be completed by analysing the cutting process. The fracture is an important parameter in all machining processes (Atkins 2003, 2005). Moreover, Atkins's idea can be applied to the analysis of the machining process, where the chip is created by shear force (Atkins 2003, 2005, 2009; Patel *et al.* 2009; Williams *et al.* 2010).

The cutting force is an energetic effect of splitting material and can be considered from the point of view of modern fracture mechanics. Such a mathematical model has been developed (Atkins 2003, 2005, 2009; Orłowski *et al.* 2017) for the description of the cutting of orthotropic materials on the basis of fracture theory and includes fracture toughness in addition to the material plasticity and friction.

Hofstetter and Gamstedt (2009) attempted to explain the relationship between the cutting force and energy using the micromechanics of deformation and wood fracture by employing new approaches and measurement techniques. Kowaluk (2007) used the application of the results obtained during longitudinal cutting and wood milling and also applied fracture mechanics to chipboard machining (Kowaluk *et al.* 2004). Orłowski and Palubicki (2009) focused on cutting by applying a macromechanics-based model. Wyeth *et al.* (2009) used Atkins' theory (Atkins 2003, 2009) for two classical cases of orthogonal wood cutting, where the first is type I chip formation, which is commonly called the chip that is formed by bending (Franz 1958; Williams 1998), and the second is the type II chip that forms by shearing. Wyeth *et al.* (2009) described the process of chip formation during orthogonal cutting with different fibre orientations and cutting heights at low and high cutting speeds. Their work allows better mechanical understanding of chip formation.

When applying a sufficient load, the wood structure is changed. The occurring changes can take many forms because of a wide range of load conditions. If the change in structure results in bond disruption and the emergence of new surfaces, it can be considered a case of fracture. Depending on the load mode, the fracture can be gradual and incremental or catastrophic and rapid. In this context, disruption is simply the point where wood cannot withstand the load (Smith *et al.* 2003).

Because the structure of wood develops during tree growth, the fracture features vary considerably, depending on how the material is oriented relative to the growth axis. There are theoretically six different directions of crack propagation for orthotropic wood. The introduced double-index system identifies all directions of crack propagation (Smith *et al.* 2003). The first letter specifies the direction perpendicular to the crack plane, and the second letter shows the direction of crack propagation. The letters L, R, and T denote the longitudinal, radial, and tangential directions. For each wood species, a large number of crack propagation methods should be taken into account because each of these six directions can be theoretically subjected to three fracture modes. Crack propagation along the fibres (RL and TL) prevails in almost all cases because of the low strength and toughness of wood perpendicular to the fibres (Pearson 1974; Nadeau 1979; Pellicane 1980).

The main aim of this paper was to develop an alternative methodology for simultaneous determination of wood fracture toughness and shear yield strength for two principal directions regarding wood grains on the basis of cutting tests performed during circular saw blade cutting for two selected wood species of Central Europe provenance.

## THEORETICAL BACKGROUND

### Methodology

Measurements were performed on a test rig (Fig. 1) by cutting with circular saw blades at the laboratory of the Department of Wood Processing Technologies of the Faculty of Forestry and Wood Technology of Mendel University (Brno, Czech Republic). This stand simulated the conditions of circular saw cutting in real operation as accurately as possible. The stand was based on the fixed stator of a DC dynamometer (3) (DS 442-2/V model Transporta, Chrudim, Czech Republic). The speed of the spindle (1), which the saw blade is mounted on, can be controlled continuously using a Leonard device up to  $n = 12,000$  rpm at a maximum torque of  $M_c = 14$  N·m. The material was fixed on a movable carriage (7), which was led towards the cut with linear guides and was fed by a ball screw (9). The screw (9) was driven by an asynchronous electric motor (8) through a frequency converter (12), controlling the material feed towards the cutting unit. The feed speed was varied in the range  $v_f = 3$  to  $22$  m·min<sup>-1</sup>.

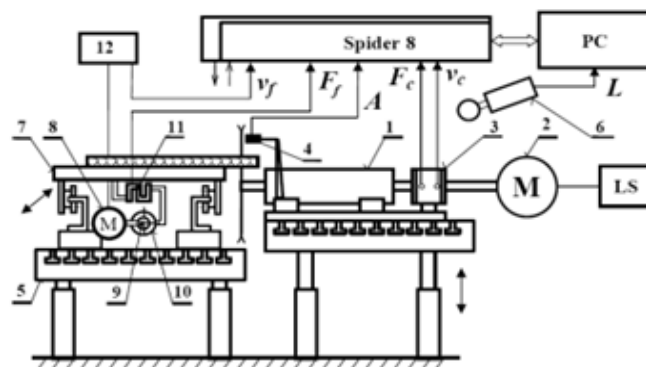


**Fig. 1.** Test stand diagram. Legend: 1 – Spindle, 2 – Dynamometer el. motor with speed control LS, 3 – Cutting force  $F_c$  and speed  $v_c$  sensor, 4 – Contactless vibration sensor A, 5 – Grate table, 6 – Noise meter, 7 – Infeed carriage, 8 – Carriage feed el. motor, 9 – Ball screw, 10 – Nut, 11 – Feed force sensor  $F_f$ , and 12 – Frequency converter for speed  $v_f$  (Kopecký *et al.* 2012)

A circular-saw blade for longitudinal wood cutting was used for this experiment (Flury Systems AG, Arch, Switzerland). It was a standard 350 mm diameter blade with straight teeth. In the cutting zone of the blade, four radial expansion grooves, ended by a copper rivet, are burned in. These grooves compensate for corrugation resulting from increased temperature and moreover reduce noise level. Further, this blade had a modified tension achieved by rolling. The design parameters of the circular-saw blade are as follows: diameter  $D = 350$  mm, teeth number  $z = 28$ , hole diameter  $d = 30$  mm, saw blade thickness  $s = 2.5$  mm, tooth height  $h = 10.5$  mm, clearance angle  $\alpha_f = 15^\circ$ , and rake angle  $\gamma_f = 20^\circ$ . The saw blade was clamped with collars 100 mm in diameter.

## Materials

Beech wood (*Fagus sylvatica* L.) samples and spruce wood (*Picea abies* (L.) Karst.) samples originating from the Training Forest Enterprise Masaryk Forest Křtiny, an organizational part of Mendel University in Brno, Czech Republic were used. The length of specimens used for the experiment was 740 mm. The thicknesses of the samples were  $e_1 = 40$  mm and  $e_2 = 50$  mm (Table 1). The width of samples varied; however, because of the manner in which the tests were conducted, this issue was insignificant. The samples were stored for 30 days in a room with constant temperature conditions of 20 °C and 50% air humidity. Moisture was detected by a humidity meter (HMB-WS25, Merlin Technology GmbH, Tumeltsham, Austria), which was used for quick non-destructive wood moisture measurements. The gravimetric method was used to more accurately determine the moisture content of the samples.

**Table 1.** Additional Information on Cutting Conditions and Materials

	Material	Moisture $w$ (%)	Cutting height $e$ (mm)						Density $\rho_w$ (kg·m <sup>-3</sup> )		
			40	50	60	70	80	90	100	110	120
Experiment No. 1: Beech40 and Spruce40	Beech	8.4	40	50	60	70	80	90	100	110	120
	Spruce	8.5	40	50	60	70	80	90	100	110	120
Experiment No. 2: Beech50 and Spruce50	Beech	8.5	50	60	70	80	90	100	110	120	
	Spruce	8.6	50	60	70	80	90	100	110	120	
Feed speed $v_f$ (m·min <sup>-1</sup> )	2	4	6	8	10	13	16	19	22		

The feed speed of the workpiece was varied in the range  $v_f = 2$  to 22 m·min<sup>-1</sup> with steps shown in Table 2. This corresponded to the feed per tooth ( $f_z$ ) and the mean uncut chip thickness ( $h_m$ ). For the present cutting conditions and each type of material, a series of measurements was subjected to statistical assessment, and 25 measurements were used for each feed speed.

### Determination of model parameters

For further calculations, it was necessary to define the cutting model. This was determined based on the technology that was used by defining individual angles between the wood fibre grain, the tool planes, and the motion vectors involved in the cutting process. In longitudinal circular saw cutting, an axial-perpendicular cutting model is used. Calculation of the kinematic elements of circular saw cutting was performed in accordance

with the following equations. The variables ( $f_z$ ,  $\varphi_2$ ,  $h_m$ ) were the input parameters for calculation of the cutting resistance, and their values are shown in Table 2.

When calculating, the mean uncut chip thickness  $h_m$  was considered. It was determined using the mean fibre cutting angle  $\varphi_2$ . From the geometry of circular-saw blade cutting, it is evident that the angle of fibre cutting varied. At the point of tooth contact with the workpiece, this angle was equal to  $\psi_1$ , and at the point of circular-saw blade teeth disengagement, it was much higher and equal to the exit angle  $\psi_2$ . The mean fibre cutting angle was then determined as the average value of both angles:

$$\psi_1 = \arccos\left(\frac{a_e + e}{R}\right), \psi_2 = \arccos\left(\frac{a_e}{R}\right), \varphi_2 = \frac{\psi_1 + \psi_2}{2} \quad (1)$$

where  $\psi_1$  is the angle of tooth entrance,  $a_e$  is the position of the workpiece,  $e$  is the workpiece height,  $R$  is the circular saw blade radius,  $\psi_2$  is exit the angle,  $\varphi_2$  is the mean fibre cutting angle

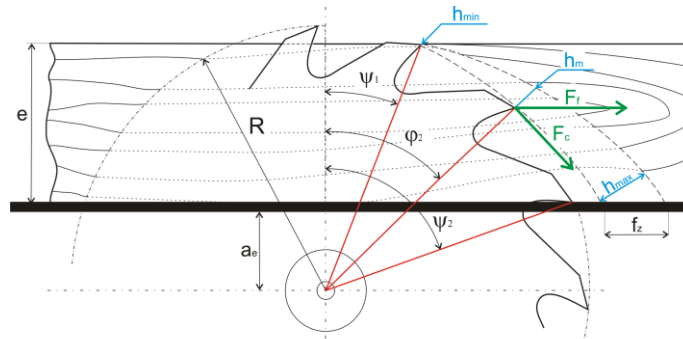


**Fig. 2.** Sawing kinematics on circular sawing machine:  $f_z$  – Feed per tooth,  $R$  – Circular saw blade radius,  $h_m$  – Mean uncut chip thickness,  $h_{min}$  – Minimum uncut chip thickness,  $h_{max}$  – Maximum uncut chip thickness,  $e$  – Workpiece height,  $a_e$  – Position of the workpiece,  $\varphi_2$  – Mean fibre cutting angle,  $\psi_1$  – Entry angle,  $\psi_2$  – Exit angle,  $F_c$  – Cutting force, and  $F_f$  – Feed force

When the tooth began to cut, the uncut chip thickness had the minimum value,  $h_{min}$ . The maximum uncut chip thickness  $h_{max}$  was reached at the moment when the tooth left the workpiece. As already mentioned, the mean uncut chip thickness  $h_m$  was considered in the calculation models. The mean uncut chip thickness was then calculated from Eq. 2,

$$h_m = f_z \cdot \sin \varphi_2 \quad (2)$$

Feed per tooth can be expressed according to the known relationship Eq. 3,

$$f_z = \frac{v_f}{n \cdot z} \quad (3)$$

where  $f_z$  is the feed per tooth,  $v_f$  is the feed speed,  $n$  is the rotation frequency of the circular-saw blade and  $z$  is the number of circular-saw blade teeth.

**Table 2.** Input Parameters for Calculation of Cutting Resistance

Experiment No. 1: Beech40 and Spruce40									
$v_f$ ( $m \cdot min^{-1}$ )	2	4	6	8	10	13	16	19	22
$f_z$ (mm)	0.0188	0.0376	0.0564	0.0752	0.094	0.1222	0.1504	0.1786	0.2068
$\varphi_2$ (°)	31.93								
$h_m$ (mm)	0.01	0.02	0.03	0.04	0.05	0.065	0.08	0.094	0.109
Experiment No. 2: Beech50 and Spruce50									
$v_f$ ( $m \cdot min^{-1}$ )	2	4	6	8	10	13	16	19	22
$f_z$ (mm)	0.0188	0.0376	0.0564	0.0752	0.094	0.1222	0.1504	0.1786	0.2068
$\varphi_2$ (°)	37.48								
$h_m$ (mm)	0.011	0.023	0.034	0.046	0.057	0.074	0.091	0.109	0.126

*Fracture mechanics-based model*

The method of determining fracture toughness and shear yield strength is based on the cutting theory originally designed by Atkins and Vincent (1984). If chips are formed by shearing, the cutting force size can be established experimentally. The relationship between the cutting force size and the uncut chip thickness is considered to be linear when cutting the majority of materials. The only exception is the zone of extremely thin chips formed when the cutting mechanism changes significantly. The same results are reported by Csanády and Magoss (2013) for processing wood and wood-based materials. This conclusion was confirmed experimentally for a sash gang saw (Orlowski 2007; Orlowski and Atkins 2007; Orlowski and Palubicki 2009) and for circular saw cutting (Kopecký *et al.* 2014, Hlásková *et al.* 2015). Therefore, it is possible to precisely describe the dependence of the cutting force on the varying uncut chip thickness, using two experimental points resulting from at least two independent measurements.

Another method for determining the fracture toughness and shear yield strength along and across the fibres has been demonstrated (Orlowski *et al.* 2017; Sandak *et al.* 2017). At least four cutting experiments should be performed. It is important to ensure that at least two different levels of feed speed  $v_f$  and two different uncut chip thicknesses  $h_m$  are used, which correspond to different cutting heights  $e$ . In general, when increasing the number of feed speed levels or cutting height levels, measurement reliability is improved. It could be emphasised that the mentioned above method, which was used by Orlowski *et al.* (2017) and Sandak *et al.* (2017), was implemented in this research.

According to the latest theoretical knowledge using fracture mechanics methods (Atkins 2003; Orlowski 2007; Orlowski *et al.* 2013), the mathematical model of power calculation for circular-saw blade cutting can be expressed by Eq. 4,

$$\bar{P}_{cw} = \left[ z_a \cdot \frac{\tau_\gamma \cdot b \cdot \gamma}{Q_{shear}} \cdot h_m \cdot v_c + z_a \cdot \frac{R \cdot b}{Q_{shear}} \cdot v_c \right] \quad (4)$$

where  $z_a$  is the number of teeth in contact with the kerf (on average),  $\tau_\gamma$  is the shear yield stress (MPa),  $b$  is the saw kerf thickness (mm),  $\gamma$  is the shear strain along the shear plane (-),  $h_m$  is the mean uncut chip thickness (mm),  $v_c$  is the cutting speed,  $R$  is the specific work required for surface separation and new surface creation (fracture toughness) ( $J \cdot m^{-2}$ ), and  $Q_{shear}$  is the friction correction (-).

In this model, chip formation consists of deformation and displacement of material sub-layers when the tool is moved into a cut, and these layers are separated in the plane,



inclined at an angle  $\Phi$ . Deformation of the machined chip material on the tool face is transferred to the free chip surface, and new surfaces are formed. A chip is *de facto* mostly in flat contact with the tool face. Shear deformation in the cutting zone differs from pure shearing by assuming the effects of compound stress-shear components and normal components. Shear strain of the chips is based on relative displacement and when modified, is defined by Eq. 5,

$$\gamma = \frac{\cos \gamma_f}{\cos(\Phi - \gamma_f) \sin \Phi} \quad (5)$$

where  $\gamma_f$  is the rake angle and  $\Phi$  is the shear plane angle, which defines the orientation of the shear plane with respect to the machined surface.

Unknown parameters in the model were set based on calculation of the forces acting on the workpiece and the tool. Using the measured cutting force  $F_c$  and the feed force  $F_f$ , other components of the resulting active force were calculated. The computation was based on Ernst-Merchant's force decomposition diagram. Using the calculated cutting force components, additional model parameters were calculated. Then, the shear plane angle  $\Phi$  was determined. For large uncut chip thicknesses, Ernst-Merchant's equation serves as the basis for large uncut chip thickness values; the shear plane angle  $\Phi$  is constant, as shown in Eq. 6,

$$\Phi = \left(\frac{\pi}{4}\right) - \left(\frac{1}{2}\right) (\beta_\mu - \gamma_f) \quad (6)$$

where  $\beta_\mu$  is the friction angle given by  $\tan^{-1} \mu = \beta_\mu$ ,  $\mu$  is the coefficient of friction.

Another parameter of the model is the friction correction  $Q_{shear}$ , which was calculated according to Eq. 7.

$$Q_{shear} = [1 - \sin \beta_\mu \cdot \sin \Phi / \cos(\beta_\mu - \gamma_f) \cos(\Phi - \gamma_f)] \quad (7)$$

The shear angle should be corrected according to the ratio of  $R$  and  $\tau_\gamma$  (Atkins 2003). It was found that shear angle values that were computed according to Eq. 6 were frequently higher than the experimentally measured values. It is important to mention that this model assumes perfect sharpness of the cutting edge. Moreover, it does not consider the effect of blunting and chip momentum resulting from the mean values of feed speeds during wood cutting. It is therefore assumed under these conditions that the cutting force  $F_c$  increases linearly with growing uncut chip thickness  $h_m$ . Under the theory which uses the fracture mechanics, the cutting force per one tooth, is expressed by the slope of the line in the form  $y = (k) \cdot x + q$ .

Orlowski *et al.* (2017) claim that based on performed experiments, the system of linear equations for  $F_c^{1z}$  and the height of the cut material  $e$  can be determined, as shown in Eq. 8,

$$\begin{cases} F_{c1}^{1z} = k_1 h_m + q_1 \\ F_{c2}^{1z} = k_2 h_m + q_2 \end{cases} \quad (8)$$

where  $F_{c1}^{1z}$  and  $F_{c2}^{1z}$  are cutting forces per one tooth, in sawing workpiece of height  $e_1$  and  $e_2$ ,  $k_1$  and  $k_2$  are slopes, and  $q_1$  and  $q_2$  are intercepts.

Orlowski and Palubicki (2009) showed that on the basis of these equations, it was possible to determine the shear yield strength values  $\tau_{\gamma||L1}(e_1)$  and  $\tau_{\gamma||L2}(e_2)$  as the slope  $k_1$  and  $k_2$ , as shown in Eq. 9,

$$k_1 = \frac{\tau_{\gamma\parallel 1} \cdot b_1 \cdot \gamma_1}{Q_{shear1}} \quad (9)$$

$$k_2 = \frac{\tau_{\gamma\parallel 2} \cdot b_2 \cdot \gamma_2}{Q_{shear2}}$$

where  $\tau_{\gamma\parallel 1}$  and  $\tau_{\gamma\parallel 2}$  are shear yield strength values,  $b_1$  and  $b_2$  are widths of cutting edges,  $\gamma_1$  and  $\gamma_2$  are shear strains along the shear plane, and  $Q_{shear1}$  and  $Q_{shear2}$  are friction corrections for height of workpiece  $e_1$  and  $e_2$ .

It is important to emphasize that all of the parameters are calculated independently for each system equation. In a similar way, the fracture toughness  $R_{\parallel 1}$  and  $R_{\parallel 2}$  is calculated as shown in Eq. 10,

$$q_1 = \frac{R_{\parallel 1} \cdot b_1}{Q_{shear1}} \quad (10)$$

$$q_2 = \frac{R_{\parallel 2} \cdot b_2}{Q_{shear2}}$$

where  $R_{\parallel 1}$  and  $R_{\parallel 2}$  are fracture toughness values, and  $q_1$  and  $q_2$  are the values of line displacement for the cutting heights  $e_1$  and  $e_2$ .

Values of fracture toughness of the material  $R_{\parallel 1}$  and  $R_{\parallel 2}$  and of the shear yield strength  $\tau_{\gamma\parallel 1}$  and  $\tau_{\gamma\parallel 2}$ , derived from Eqs. 9 and 10, can be applied neither in the parallel nor the perpendicular direction with respect to the fibres. Therefore, it is necessary to calculate an explicit value for each of the specific characteristics of the material. Orlicz (1998) used a transformation equation of the flat stress to determine the specific cutting resistance for the axial-perpendicular model of cutting. The same method is commonly used in the general mechanics of materials for transformation of individual stress components (Gere 2004). The following system of equations provides a mathematical basis for calculating model parameters with respect to the influence of the fibre cutting angle. As shearing is performed in the shear plane, the value of the shear plane angle was taken into account in Eqs. 11 and 12,

$$\begin{cases} \tau_{\gamma\parallel 1} = \tau_{\gamma\parallel} \cos^2(\varphi_{21} + \Phi_1) + \tau_{\gamma\perp} \sin^2(\varphi_{21} + \Phi_1) \\ \tau_{\gamma\parallel 2} = \tau_{\gamma\parallel} \cos^2(\varphi_{22} + \Phi_2) + \tau_{\gamma\perp} \sin^2(\varphi_{22} + \Phi_2) \end{cases} \quad (11)$$

$$\begin{cases} R_{\parallel 1} = R_{\parallel} \cos^2 \varphi_{21} + R_{\perp} \sin^2 \varphi_{21} \\ R_{\parallel 2} = R_{\parallel} \cos^2 \varphi_{22} + R_{\perp} \sin^2 \varphi_{22} \end{cases} \quad (12)$$

where  $\tau_{\gamma\parallel}$  is the shear yield strength along the fibre direction (MPa),  $\tau_{\gamma\perp}$  is the shear yield strength perpendicular to the fibres (MPa),  $R_{\parallel}$  is the fracture toughness along the fibre direction ( $\text{J}\cdot\text{m}^{-2}$ ), and  $R_{\perp}$  is the fracture toughness perpendicular to the fibres ( $\text{J}\cdot\text{m}^{-2}$ ).

Orlowski *et al.* (2013) demonstrated that fracture toughness  $R_{\parallel}$  and shear yield strength  $\tau_{\gamma\parallel}$  for combined cutting models can be calculated based on  $R_{\perp}$  and  $\tau_{\gamma\perp}$ . Both parameters ( $R_{\perp}$  and  $\tau_{\perp}$ ) were determined empirically during the experiment that focused on cross cutting (Orlowski and Palubicki 2009). Fracture toughness  $R_{\parallel}$  and shear yield strength  $\tau_{\gamma\parallel}$  values in the longitudinal direction were calculated using corresponding coefficients obtained from the literature. Kopecký *et al.* (2014) developed an alternative method for the determination of  $R_{\parallel}$  and  $\tau_{\gamma\parallel}$  of orthotropic materials when machining with a circular saw. Both values were suitable only for a given cutting edge direction, which is characterized by the mean value of the fibre cutting angle  $\varphi_2$  and cannot be considered material constants (Orlowski *et al.* 2017). Hlásková *et al.* (2015) proposed a combined method for the determination of fracture toughness and strength parameters for basic cutting-edge



positions for the longitudinal and perpendicular directions of cutting. However, the main drawback of this method is that two types of machine tools with different kinematics are required.

## RESULTS

To determine the fracture toughness of the material  $R_{\parallel}$  and  $R_{\perp}$  and shear yield strength  $\tau_{\gamma\parallel}$  and  $\tau_{\gamma\perp}$  (for longitudinal and perpendicular cutting) of orthotropic materials, it is necessary to ensure different feed speeds  $v_f$  and at least two different cutting heights  $e$ . To verify this method, the results obtained when cutting spruce and beech samples at two different cutting heights ( $e_1 = 40$  mm,  $e_2 = 50$  mm) were applied.

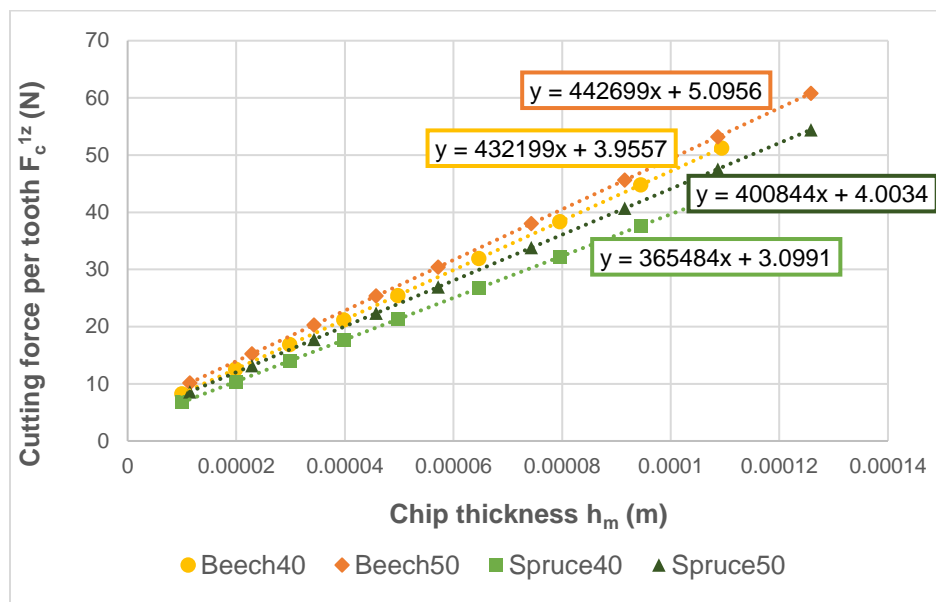


Fig. 3. Cutting force per tooth versus average uncut chip thickness while circular sawing

### Beech

Based on the performed experiments, a system of linear equations was determined for beech wood, namely for  $F_c^{1z}$  and for the thicknesses of the cut material  $e_1 = 40$  mm and  $e_2 = 50$  mm.

$$\begin{aligned} F_{c1}^{1z}(\varphi_{21} = 31.94^\circ) &= 432199h_m + 3.9557 \\ F_{c2}^{1z}(\varphi_{22} = 37.48^\circ) &= 442699h_m + 5.0956 \end{aligned} \quad (13)$$

The qualities of the regression models were characterized by the coefficients of determination. The values corresponding to models presented in Fig. 3 were  $r^2 = 0.99$  for thickness  $e_1$  and  $r^2 = 0.99$  for  $e_2$  thickness.

Determination of the main parameters of the model was based on the regression analysis. Fracture toughness  $R_{\parallel\perp}$  was determined from line displacement, and shear yield strength  $\tau_{\gamma\parallel\perp}$  was determined from the gradient. The following parameters of the model were calculated for the axial-perpendicular model of cutting (Table 3).

**Table 3.** Input Data for New Model of Computation, Beech (*Fagus sylvatica* L.)

	$\varphi_2$ (°)	$\mu$ (-)	$\beta_\mu$ (°)	$\Phi$ (°)	$\gamma$ (-)	$Q_{shear}$ (-)	$\tau_{\gamma\perp}$ (MPa)	$R_{\perp}$ (J·m <sup>-2</sup> )
Beech40	31.94	0.63	33.56	38.22	1.60	0.63	47.27	1098.81
Beech50	37.48	0.63	31.01	39.495	1.57	0.65	50.67	1415.44

For calculation of the fracture toughness in two main directions of cutting, a set of linear equations with two unknowns, as shown in Eq. 14, was used. For calculation of the shear yield strength, a system of linear equations with two unknowns, as shown in Eq. 15, was used. The resulting values are shown in Table 4.

$$47.27 = \tau_{\gamma\parallel} \cos^2(31.94 + 38.22) + \tau_{\gamma\perp} \sin^2(31.94 + 38.22) \quad (14)$$

$$50.67 = \tau_{\gamma\parallel} \cos^2(37.48 + 39.495) + \tau_{\gamma\perp} \sin^2(37.48 + 39.495)$$

$$1098.81 = R_{\parallel} \cos^2 31.94 + R_{\perp} \sin^2 31.94 \quad (15)$$

$$1415.44 = R_{\parallel} \cos^2 37.48 + R_{\perp} \sin^2 37.48$$

**Table 4.** Fracture Toughness and Shear Yield Strength for Beech (*Fagus sylvatica* L.)

$R_{\parallel}$ (J·m <sup>-2</sup> )	$R_{\perp}$ (J·m <sup>-2</sup> )	$R_{\parallel}/R_{\perp}$	$\tau_{\gamma\parallel}$ (MPa)	$\tau_{\gamma\perp}$ (MPa)	$\tau_{\gamma\parallel}/\tau_{\gamma\perp}$
114.0	3629.1	0.031	11.86	49.87	0.238

### Spruce

Based on the performed experiments, the system of linear equations was determined for spruce wood, namely for  $F_c^{1z}$  and for heights of the cut material  $e_1 = 40$  mm and  $e_2 = 50$  mm.

$$F_{c1}^{1z}(\varphi_{21} = 31.94^\circ) = 365484h_m + 3.0991 \quad (16)$$

$$F_{c2}^{1z}(\varphi_{22} = 37.48^\circ) = 400844h_m + 4.0034$$

The qualities of the regression models were characterized by the coefficients of determination. The values corresponding to models presented in Fig. 3 were  $r^2 = 0.99$  for  $e_1$  thickness and  $r^2 = 0.99$  for  $e_2$  thickness.

Determination of the main parameters of the model was based on the regression analysis. The following parameters of the model was calculated for the axial-perpendicular model of cutting (see Table 5).

**Table 5.** Input Data of the New Model of Computation, Spruce (*Picea abies* (L.) Karst.)

(°)	$\varphi_2$ (°)	$\mu$ (-)	$\beta_\mu$ (°)	$\Phi$ (°)	$\gamma$ (-)	$Q_{shear}$ (-)	$\tau_{\gamma\perp}$ (MPa)	$R_{\perp}$ (J·m <sup>-2</sup> )
Spruce40	31.94	0.7	33.82	38.09	1.60	0.63	39.79	860.86
Spruce50	37.48	0.7	36.31	36.85	1.64	0.61	41.72	1112.06

For calculation of the fracture toughness in the two main directions of cutting, a set of linear equations with two unknowns, as shown in Eq. 17, was used. For calculation of the shear yield strength, a set of linear equations with two unknowns, as shown in Eq. 18, was used. The resulting values are shown in Table 6.

$$39.79 = \tau_{\gamma\parallel} \cos^2(31.94 + 38.09) + \tau_{\gamma\perp} \sin^2(31.94 + 38.09) \quad (17)$$

$$41.72 = \tau_{\gamma\parallel} \cos^2(37.48 + 36.85) + \tau_{\gamma\perp} \sin^2(37.48 + 36.85)$$

$$860.86 = R_{\parallel} \cos^2 31.94 + R_{\perp} \sin^2 31.94 \quad (18)$$

$$1112.06 = R_{\parallel} \cos^2 37.48 + R_{\perp} \sin^2 37.48$$

**Table 6.** Fracture Toughness and Shear Yield Strength for Spruce (*Picea abies* (L.) Karst.)

$R_{\parallel}$ (J·m <sup>-2</sup> )	$R_{\perp}$ (J·m <sup>-2</sup> )	$R_{\parallel}/R_{\perp}$	$\tau_{\gamma\parallel}$ (MPa)	$\tau_{\gamma\perp}$ (MPa)	$\tau_{\gamma\parallel}/\tau_{\gamma\perp}$
82.5	2863.8	0.029	12.08	40.73	0.297

## DISCUSSION

### Beech

Based on the performed experiments and Ernst-Merchant's theory for saw blade cutting conditions, the input parameters for beech machining were determined as shown in Table 3. Based on these parameters, it was possible to determine the shear yield strength for two different cutting heights, characterised by the fibre cutting angle:  $\tau_{\gamma\perp}$  (31.94°) = 47.27 MPa and  $\tau_{\gamma\parallel}$  (37.48°) = 50.67 MPa. The calculated values of the fracture toughness  $R_{\parallel\perp}$  were as follows:  $R_{\parallel\perp}$  (31.94°) = 1098.81 J·m<sup>-2</sup> and  $R_{\parallel\perp}$  (37.48°) = 1415.44 J·m<sup>-2</sup>. Table 4 converts these values for two basic anatomic directions (Orlowski *et al.* 2017): parallel to fibres  $\tau_{\gamma\parallel}$  = 11.86 MPa and perpendicular to fibres  $\tau_{\gamma\perp}$  = 49.87 MPa. By comparing these results with corresponding values of reference experiments (Hlásková *et al.* 2015), where the following is valid for beech ( $\tau_{\gamma\perp}$  = 43.86 MPa), it follows that the values according to the newly designed method were higher by 6 MPa.

The  $\tau_{\gamma\parallel}/\tau_{\gamma\perp}$  ratio was determined from the experimental measurements. The ratio was 0.238. In the reference materials, the ratio was 0.29. It is worth mentioning that the reference value  $\tau_{\gamma\parallel}$  = 13 MPa was determined based on the modulus of rupture (MOR) obtained during static bending. Orlowski *et al.* (2013; 2017) claim that the  $\tau_{\gamma\parallel}$  value can be estimated on the MOR basis, where  $\tau_{\gamma\parallel}$  = 0.125·MOR. In this study the MOR = 104.3 MPa (Papadopoulos 2008). Different values of  $\tau_{\gamma\parallel}/\tau_{\gamma\perp}$  ratios can be explained by various methodological procedures and the different origins of the studied materials (Chuchala *et al.* 2014). Kretschmann (2010) claims that the shear yield strength of the wood parallel to the fibres ranges from 3 MPa to 15 MPa at 12% moisture, depending on the origin of the material and on the growth conditions. Green (2001) states in his work that because of the orthotropic wood features, it is very difficult to obtain results for the cut perpendicular to the fibres. A small amount of data suggests that the shear yield strength perpendicular to the fibres can be 2.5 times to 3 times higher than the shear yield strength parallel to the fibres. Orlowski *et al.* (2017) shows that the  $\tau_{\gamma\perp}/\tau_{\gamma\parallel}$  = 3.44 ratio when pine was machined on a circular saw. According to this experimental examination, the value of this ratio for beech machining was  $\tau_{\gamma\perp}/\tau_{\gamma\parallel}$  = 4.2. Blackman *et al.* (2013) and Wang *et al.* (2013) claim that shear yield strength values  $\tau_{\gamma}$ , obtained on the basis of performed cutting test, can be higher than values, obtained on the basis of fracture tests. Wood is a complex natural composite with three natural polymers that have different mechanical features, where each affects the cutting process. When machining, the cutting-edge contacts the anatomical

elements and compresses them. This may lead in some cases to increased shear yield strength values.

Table 4 also shows values of the fracture toughness parallel to fibres of  $R_{\parallel} = 114 \text{ J}\cdot\text{m}^{-2}$  and perpendicular to fibres  $R_{\perp} = 3629.1 \text{ J}\cdot\text{m}^{-2}$ . Comparison of these results with the reference samples (Hlásková *et al.* 2015), where  $R_{\parallel} = 23.3 \text{ J}\cdot\text{m}^{-2}$  and  $R_{\perp} = 3886 \text{ J}\cdot\text{m}^{-2}$ , shows that the fracture toughness perpendicular to fibres values are comparable, although the  $R_{\parallel}/R_{\perp}$  ratio was lower ( $R_{\parallel}/R_{\perp} = 0.005$ ) when compared with the newly designed methodology ( $R_{\parallel}/R_{\perp} = 0.031$ ). These results are close to the values of the research performed by Orłowski *et al.* (2017), where the ratio for pine was  $R_{\parallel}/R_{\perp} = 0.017$ . There is a lack of reference data; therefore, reference values were again determined on the basis of cutting tests in combination with the results obtained by static bending and those taken from the literature. The differences in the origin of the samples and their physical features are important factors affecting the differences observed in the experimental results. It is worth mentioning that there are very few available reference values related to the fracture properties of wood (Orłowski *et al.* 2017).

### Spruce

The same methodology was used to determine the input parameters for spruce processing (Table 5). Based on these parameters, it was possible to determine shear yield strength for two different cutting heights, characterized by the fibre cutting angle:  $\tau_{\gamma\perp}$  ( $31.94^{\circ}$ ) = 39.79 MPa and  $\tau_{\gamma\parallel}$  ( $37.48^{\circ}$ ) = 41.72 MPa. Calculated values of the fracture toughness  $R_{\perp\parallel}$  were obtained as follows:  $R_{\perp\parallel}$  ( $31.94^{\circ}$ ) = 860.86  $\text{J}\cdot\text{m}^{-2}$  and  $R_{\perp\parallel}$  ( $37.48^{\circ}$ ) = 1112.06  $\text{J}\cdot\text{m}^{-2}$ .

Table 6 shows the converted values for two basic anatomic directions: parallel to fibres  $\tau_{\gamma\parallel} = 12.08 \text{ MPa}$  and perpendicular to fibres  $\tau_{\gamma\perp} = 40.73 \text{ MPa}$ . Kretschmann (2010) shows in his work the  $\tau_{\gamma\parallel}$  values for different spruce species ranging from 6.7 to 8.9 MPa at 12% moisture. Green (2001) claims that the shear yield strength along the fibres for the Sitka spruce (at  $w = 12\%$ ) is  $\tau_{\gamma\parallel} = 7.9 \text{ MPa}$ . The  $\tau_{\gamma\parallel}/\tau_{\gamma\perp}$  ratio, equalling to 0.297, was calculated from experimental measurements. In case of spruce, it is difficult to deduce a clean cut perpendicular to the fibres; therefore, there is a lack of reference data in this respect. Green (2001) claims that the shear yield strength of wood perpendicular to the fibres is up to three times higher than the shear yield strength parallel to the fibres. The reference value  $\tau_{\gamma\parallel} = 8.25 \text{ MPa}$  was determined on the basis of the modulus of rupture (MOR) obtained during static bending (Lavers 1983). Based on Green's (2001) claims, the reference value of the shear yield strength perpendicular to fibres has been calculated, namely  $\tau_{\gamma\perp} = 24.75 \text{ MPa}$ . The  $\tau_{\gamma\parallel}/\tau_{\gamma\perp}$  ratio, equal to 0.33, has been calculated from the reference values. The reference values were determined by static bending tests and were also taken from the literature, and this way we can clarify differences in values compared with the experimental data. The ratio  $\tau_{\gamma\perp}/\tau_{\gamma\parallel} = 3.37$  follows from experimental examinations during spruce sample cutting on a circular saw. Orłowski *et al.* (2017) in his work shows the ratio  $\tau_{\gamma\perp}/\tau_{\gamma\parallel} = 3.44$  when pine was machined on a circular saw. This fact conforms to the claims of Green (2001) that the shear yield strength perpendicular to fibres can be three times higher than that along the fibres.

Table 6 also shows values of fracture toughness parallel to fibres  $R_{\parallel} = 82.5 \text{ J}\cdot\text{m}^{-2}$  and perpendicular to fibres  $R_{\perp} = 2863.8 \text{ J}\cdot\text{m}^{-2}$ . Comparison of these results with the reference data is impossible because reference values of fracture wood features are unavailable for spruce samples. The ratio of fracture toughness parallel to fibres and



perpendicular to fibres is  $R_{\parallel}/R_{\perp} = 0.029$ . Orłowski and Ochrymiuk (2017) determined the ratio for pine, namely:  $R_{\parallel}/R_{\perp} = 0.029$ . Machining involves multiple physical processes and, because of the orthotropic character of wood, it is very difficult to create a clean cut, as fracture and deformation occur in different fracture modes and combinations of them. Deduction and comparison of fracture toughness values based on the results obtained by static bending is therefore problematic.

## CONCLUSIONS

1. Application of the results obtained in the experiment allowed the determination of the fracture toughness and shear yield strength of sawn wood for the axial-perpendicular model of cutting by a circular-saw blade, even though cutting wood with a circular saw is not an example of pure orthogonal cutting. Both parameters were suitable for the given direction of cutting edge movement and were not considered constants. Alternatively, these parameters can be converted by the novel method for two principal directions regarding wood grains, where they can be considered non-variable features.
2. The results of the demonstration tests revealed that for beech wood, the ratios  $R_{\parallel}/R_{\perp} = 0.031$  and  $\tau_{\gamma\parallel}/\tau_{\gamma\perp} = 0.238$ , and for spruce wood, the ratios  $R_{\parallel}/R_{\perp} = 0.029$  and  $\tau_{\gamma\parallel}/\tau_{\gamma\perp} = 0.297$ . The computed values were slightly different than the values reported in literature, but this can be explained by the methodological differences in the determination methods.
3. Various methods on how to calculate the fracture toughness were found in the literature. Unfortunately, the majority of these methods were intended for isotropic materials, or the fracture toughness was calculated based on the performed fracture tests. Using the newly designed model, it was possible to determine fracture toughness and shear yield strength only on the basis of cutting tests, without performing complex fracture tests.
4. The methodology presented can be, after slight adaptations, applied to a wide range of materials (wood-based materials and modified industrial materials) during processing on other machines with different cutting kinematics, such as routers, bandsaws, and sash gang saws (in case in which rake angle does not exceed 35 deg, when in the cutting zone shear is observed (Franz 1958)). The model is available not only for woodworking engineers dealing with woodworking processes, but also for designers when designing new saw blades or sawing machines.

## ACKNOWLEDGMENTS

This article is based on research sponsored by the Internal Grant Agency FFWT of Mendel University (Brno, Czech Republic). The authors are grateful for the support of the application of progressive technologies, which deal with unconventional material machining (Grant IGA No. LDF\_PSV\_2016019).

## REFERENCES CITED

- Atkins, A. G. (2003). "Modelling metal cutting using modern ductile fracture mechanics: Quantitative explanations for some longstanding problems," *International Journal of Mechanical Sciences* 45(2), 373-396. DOI: 10.1016/S0020-7403(03)00040-7
- Atkins, A. G. (2005). "Toughness and cutting: A new way of simultaneously determining ductile fracture toughness and strength," *Engineering Fracture Mechanics* 72(6), 849-860. DOI: 10.1016/j.engfracmech.2004.07.014
- Atkins, A. G. (2009). *The Science and Engineering of Cutting. The Mechanics and Process of Separating, Scratching and Puncturing Biomaterials, Metals and Non-Metals*, Butterworth-Heinemann, Oxford, UK.
- Atkins, A. G., and Vincent, J. F. V. (1984). "An instrumented microtome for improved histological sections and the measurement of fracture toughness," *Journal of Materials Science Letters* 3, 310-312.
- Blackman, B. R. K., Hoult, T. R., Patel, Y., and Williams, J. G. (2013). "Tool sharpness as a factor in machining tests to determine toughness," *Engineering Fracture Mechanics* 101, 47-58. DOI: 10.1016/j.engfracmech.2012.09.020
- Buršíková, V., Sťahel, P., Navrátil, Z., Buršík, J., and Janča, J. (2004). *Surface Energy Evaluation of Plasma Treated Materials by Contact Angle Measurement*, Masaryk University, Brno, CZ.
- Chuchala, D., Orłowski, K., Sandak, A., Sandak, J., Pauliny, D., and Barański, J. (2014). "The effect of wood provenance and density on cutting forces while sawing Scots pine (*Pinus sylvestris* L.)," *BioResources* 9(3), 5349-5361. DOI: 10.15376/biores.9.3.5349-5361
- Csanády, E., and Magoss, E. (2013). *Mechanics of Wood Machining*, Springer, Berlin, Germany. DOI: 10.1007/978-3-642-29955-1
- Franz, N. C. (1958). *An Analysis of the Wood-Cutting Process*, The University of Michigan Press, Ann Arbor.
- Gere, J. M. (2004). "Mechanics of materials," *Thomson Learning Inc.*, (<http://www.hljp.edu.cn/attachment/20120820084627006.pdf>), accessed 29 June 2016.
- Green, D. W. (2001). "Wood: Strength and stiffness," in: *Encyclopedia of Materials: Science and Technology*, K. H. J. Buschow, R. W. Cahn, M. C. Flemings, B. Ilshner, E. J. Kramer, and S. Mahajan (eds.), Elsevier Science Ltd., pp. 9732-9736.
- Hlásková, L., Orłowski, K. A., Kopecký, Z., and Jedinák, M. (2015). "Sawing processes as a way of determining fracture toughness and shear yield stresses of wood," *BioResources* 10(3), 5381-94. DOI: 10.15376/biores.10.3.5381-5394
- Hofstetter, K., and Gamstedt, E. K. (2009). "Hierarchical modelling of microstructural effects on mechanical properties of wood. A review. COST Action E35 2004-2008: Wood machining - micromechanics and fracture," *Holzforschung* 63(2), 130-138. DOI: 10.1515/HF.2009.018
- Jeronimidis, G. (2000). "Fracture energy of wood: Cutting measurement and mechanisms," in: *Proceedings of the International Symposium on Wood Machining: Properties of Wood and Wood Composites Related to Wood Machining*, 27-29 September, Vienna, Austria, pp 21-29.
- Kopecký, Z., and Rousek, M. (2012). "Impact of dominant vibrations on noise level of dimension circular sawblades," *Wood Research* 57(1), 151-160.





- Kopecký, Z., Hlaskova, L., and Orłowski, K. (2014). "An innovative approach to prediction energetic effects of wood cutting process with circular-saw blades," *Wood Research* 59(5), 827-834.
- Kowaluk, G. (2007). "Application of the theory of work of cutting distribution in milling," *Electronic Journal of Polish Agricultural Universities* 10(3), 1-8.
- Kowaluk, G., Dziurka, D., Beer, P., Sinn, G., and Stanzl-Tschegg, S. (2004). "Influence of ammonia on particleboard properties," in: *Proceedings of the 2<sup>nd</sup> International Symposium on Wood Machining*, 5-7 July 2004, Vienna, Austria, pp. 459-465.
- Kretschmann, D. E. (2010). "Mechanical properties of wood," in: *Wood Handbook, Wood as an Engineering Material (FPLGTR-190)*, Department of Agriculture, Forest Service, Forest Products Lab, Madison, p. 508.
- Lavers, G. M. (1983). *The Strength Properties of Timber*. Department of the Environment, Building Research Establishment, HMSO, London, UK, 60 p.
- Nadeau, J. S. (1979). "Fracture mechanics: An overview," in: *Proceeding of 1st International Conference on Wood Fracture*, Banff, Alberta, Canada, pp. 175-186.
- Orlicz, T. (1988). *Obróbka drewna narzędziami tnącymi* (In Polish, *Wood Machining with Cutting Tools*), Warsaw University of Life Sciences Press, Warsaw, Poland.
- Orłowski, K. (2007). "Experimental studies on specific cutting resistance while cutting with narrow-kerf saws," *Advances in Manufacturing Science and Technology* 31(1), 49-63.
- Orłowski, K. A., and Atkins, A. (2007). "Determination of the cutting power of the sawing process using both preliminary sawing data and modern fracture mechanics," in: *Proceedings of the Third International Symposium on Wood Machining. Fracture Mechanics and Micromechanics of Wood and Wood Composites with Regard to Wood Machining*, 21-23 May, Lausanne, Switzerland, pp. 171-174.
- Orłowski, K. A., and Ochrymiuk, T. (2017). "A newly-developed model for predicting cutting power during wood sawing with circular saw blades," *Maderas-Ciencia y Tecnologia* 19(2), 149-162. DOI: 10.4067/S0718-221X2017005000013
- Orłowski, K. A., and Pałubicki, B. (2009). "Recent progress in research on the cutting process of wood. A review COST Action E35 2004-2008: Wood machining-micromechanics and fracture," *Holzforschung* 63(2), 181-185. DOI: 10.1515/HF.2009.015
- Orłowski, K., Ochrymiuk, T., Atkins, A., and Chuchala, D. (2013). "Application of fracture mechanics for energetic effects predictions while wood sawing," *Wood Science and Technology* 47(5), 949-963. DOI: 10.1007/s00226-013-0551-x
- Orłowski, K. A., Ochrymiuk, T., Sandak, J., and Sandak, A. (2017). "Estimation of fracture toughness and shear yield stress of orthotropic materials in cutting with rotating tools," *Engineering Fracture Mechanics* 178(2017), 433-444. DOI: 10.1016/j.engfracmech.2017.02.023
- Papadopoulos, A. (2008). "The effect of acetylation on bending strength of finger jointed beech wood (*Fagus sylvatica* L.)," *Holz als Roh-und Werkstoff* 66(4), 309-310. DOI: 10.1007/s00107-007-0223-3
- Parhizgar, S., Zachary, L. W., and Sun, C. T. (1982). "Application of the principles of linear fracture mechanics to the composite materials," *International Journal of Fracture* 20(1), 3-15. DOI: 10.1007/BF00942161
- Patel, Y., Blackman, B. R. K., and Williams, J. G. (2009). "Measuring fracture toughness from machining tests," *Proceedings of the Institution of Mechanical Engineers, Part C: Journal of Mechanical Engineering Science* 223(12), 2861-2869.

DOI: 10.1243/09544062JMES1497

Pearson, R. G. (1974). "Application of fracture mechanics to the study of the tensile strength of structural lumber," *Holzforschung* 28(1), 11-19.

DOI: 10.1007/BF00195265

Pellicane, P. J. (1980). *Ultimate Tensile Strength Analysis of Wood*, Ph.D. Dissertation, Department of Forest and Wood Science, Colorado State University, Ft. Collins, CO.

Reuleaux, F. (1900). "About the Taylor tulle white tool steel. Society for the promotion of trade diligence in Prussia," *Sitzungsberichte* 79(1), 179-220.

Sandak, J., Orłowski K. A., Ochrymiuk T., Sandak A., and Riggio M. (2017). "Report for the Short Term Scientific Mission within COST Action FP1101: Development of the in-field sensor for estimation of fracture toughness and shear strength by measuring cutting forces," *International Wood Products Journal* 8(1), 34-38.

DOI: 10.1080/20426445.2016.1232912

Smith, I., Landis, E., and Gong, M. (2003). *Fracture and Fatigue in Wood*, John Wiley and Sons, Ltd., Chichester, England.

Triboulot, P., Jodin, P., and Pluvinage, G. (1984). "Validity of fracture mechanics concepts applied to wood by finite element calculations," *Wood Science and Technology* 18(1), 51-58. DOI: 10.1007/BF00195265

Wang, H., Chang, L., Ye, L., and Williams, J. G. (2013). "Micro-cutting tests: A new way to measure the fracture toughness and yield stress of polymeric nanocomposites," in: *Proceedings of the 13th International Conference on Fracture*, 16-21 June, Beijing, China.

Williams, J. G. (1998). "Friction and plasticity effects in wedge splitting and cutting fracture tests," *Journal of Materials Science*, 33(22), 5351-5357.

DOI: 10.1023/A:100449001

Williams, J. G., Patel, Y., and Blackman B. R. K. (2010). "A fracture mechanics analysis of cutting and machining," *Engineering Fracture Mechanics*. 77(2), 293-308.

DOI: 10.1016/j.engfracmech.2009.06.011

Wyeth, D. J., Goli, G., and Atkins, A. G. (2009). "Fracture toughness, chip types and mechanics of cutting wood. A review COST Action E35 2004-2008: Wood machining - Micromechanics and fracture," *Holzforschung* 63(2), 168-180.

DOI: 10.1515/HF.2009.017

Article submitted: April 6, 2018; Peer review completed: June 15, 2018; Revisions accepted: June 21, 2018; Published: June 22, 2018.

DOI: 10.15376/biores.13.3.6171-6186